# An Effective Way to Combine Radial and Axial Magnetic Bearings in a Unit


Ha-Yong Kim
*R&D Team Servo&Mecha Group, Storage System Division*
*Samsung Electronics Co., LTD*
*Suwon, Gyeonggi, 443-742 Korea*
*hayongtk.kim@samsung.com*

Seung-Jong Kim
*Tribology Research Center*
*Korea Institute of Science and Technology*
*39-1 Hawolgok, Sungbuk, Seoul, 136-791 Korea*
*sjongkim@kist.re.kr*



***Abstract* – This paper proposes a new way to combine radial and axial active magnetic bearings in a unit. The proposed active magnetic bearing(AMB) has no large axial disk and instead use the Lorentz force for axial control. Thus this AMB system can be more compact. Its structure is basically similar to the homopolar AMB with four cores circumferentially connected by yokes. But it has two-layer windings for radial and axial controls; one is configured like a homopolar AMB, and the other is the same as that of a 4-pole heteropolar AMB. Since each winding can be used for radial control, the proposed system has two kinds of operating principle according to the radial control type. As for axial control action, it uses the Lorentz force generated by the interaction of the bias flux for radial control and the axial control flux. The feasibility of this scheme is experimentally verified by using a simple PD controller with a feedforward loop.**



***Index Terms* – Active magnetic bearing, Combined radial and axial bearings, Lorentz-type axial bearing, Axial-diskless magnetic bearing.**


## I. INTRODUCTION

For the application of AMB in various industrial fields, more compact, less expensive and simple-structured AMBs are required. Especially to make the system small and compact, the conventional axial AMB with a disk placed between two axial electromagnets should be improved, because the large diameter of the axial disk limits the maximum rotational speed and such an axial magnetic bearing makes the system large and in addition, makes the fabrication so troublesome. Thus, so far, many researchers have attempted to remove the axial disk. One of them is a cone-shaped magnetic bearing [1], [2], but it is not the ultimate solution for small size, even if it has no axial disk. As the most compact AMB, a miniaturized AMB with solid cores has also been developed [3], [4]. For compactness, such a magnetic bearing including permanent magnets for passive levitation is advantageous, but a low damping is its weak point that should be considered for practical use. On the other hand, a diskless axial AMB using the Lorentz force has been proposed recently [5], [6]. But since they are based on the hybrid AMB, inevitably they require at least two magnetic bearing units using the bias magnetic flux by permanent magnet in common.

In this paper, a new design for small-sized AMB is introduced, which enables the radial and axial control in one bearing unit without the axial disk. It consists of four U-shaped cores circumferentially connected by yokes and two-layer windings for radial and axial controls; one is configured like a homopolar AMB, and the other is the same as that of a 4-pole heteropolar AMB. Since either winding can be used for radial control, the proposed system has two kinds of operating principle according to the radial control type; coupled and uncoupled bias flux types. For radial control, the control flux is added to or subtracted from the bias flux, which results in radial Maxwell force to return the rotor to a center position. Meanwhile, for axial control, it uses the Lorentz force generated by the interaction of the bias flux for radial control and the axial control flux. In this paper, we first introduce the basic structure and the two operating principles and then theoretically derive the expressions for radial and axial electromagnetic forces based on the magnetic circuit analysis. By using a simple decentralized PD controller with a feed-forward loop for the compensation of a coupled effect, the rotor was successfully levitated. The experimental results are shown to validate the analytical findings and evaluate the performance of the newly designed AMB.

## II. STRUCTURE AND OPERATING PRINCIPLE

Fig. 1 shows the structure of the proposed AMB that has a configuration of a conventional homopolar AMB with

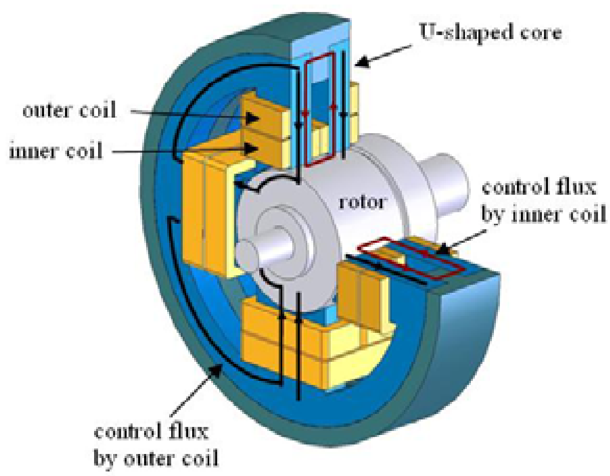


Fig. 1 Structure of the proposed AMB

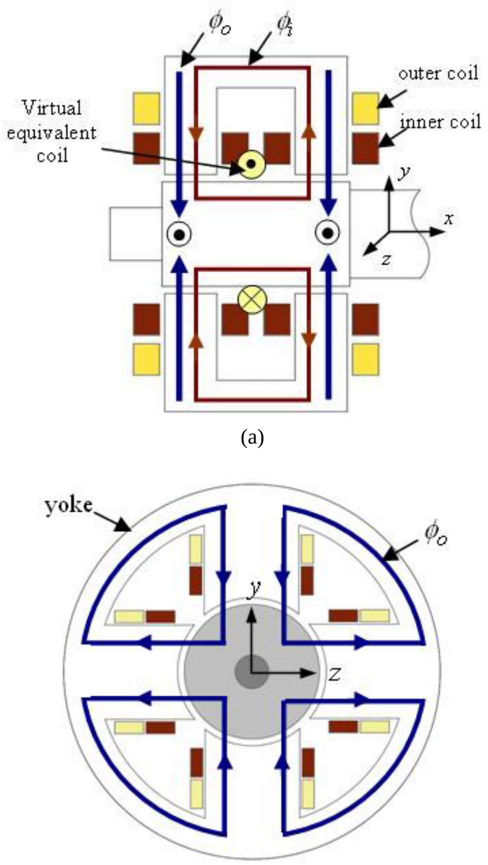


(a)

(b)

Fig. 2 Magnetic flux flow; (a) side view, (b) front view

cores circumferentially connected to each other, or in other words, a configuration of a four-pole heteropolar AMB where each core is divided in two axially. The cores have two-layer coil windings; one(marked as 'inner coil' in the figure) makes a magnetic flux flow in each U-shaped core independently and the other(marked as 'outer coil') generates a flux flowing through adjacent cores. Here, it is important to note that either of the windings can be used for the radial control, which depends on what coil the bias current flows in. When the outer coil is used for radial control, it works just like a four-pole AMB. In this case, the bias flux as well as the radial control flux flow on the plane perpendicular to the shaft axis as shown in Fig. 2(b), that is, *the bias fluxes for y- and z-directional controls are coupled*. Meanwhile, the axial control flux produced by the inner coil flows in the path composed of a U-shaped core, air gaps, and rotor, as shown in Fig. 2(a). Then, the inner coil can be regarded as a virtual coil in the magnetic field produced by the bias flux. Therefore, the Lorentz force acts on the coil, which results in axial force reacting on the rotor because the coil is fixed in the core. This is the key idea that this paper proposes. The direction and strength of the axial force can be controlled by the axial control current.

On the other hand, when the inner coil is used for radial control, its levitation principle is very similar to that of the conventional homopolar AMB. But actually, it should be heteropolar, that is, the rotor experiences four *N*, *S*, *N*, *S*-pole cores in turn during a rotation. In other words, the direction of $\phi_i$ of Fig. 2(a) is different from that of the adjacent cores. This is so as to generate the axial force in the same direction at the cores when the flux $\phi_o$ is applied. In this case, note that *the bias fluxes generated by four cores have independent paths*. From an axial-control point of view, we can consider that the outer coil makes a magnetic field where a virtual coil with bias current lies. Thus the Lorentz force is generated again, which can be controlled by the field. Hereafter, for these two configurations, magnetic circuit analysis and some levitation experimental results are introduced.

## III. Magnetic Force Analysis

One of the magnetic fluxes, $\phi_o$ and $\phi_i$ as shown in Fig. 2(a), corresponds to the radial control flux, $\phi_{cr}$, with bias flux, $\phi_b$, and the other is the axial control flux, $\phi_{cx}$. Even whichever is in charge of the radial control, the radial force in *y* direction can be expressed as

$$F_y = \frac{(\phi_b+\phi_{cr})_I^2 - (\phi_b-\phi_{cr})_{III}^2 + (\phi_{cx})^2{}_I - (\phi_{cx})^2{}_{III}}{\mu_o A_g} = \frac{1}{\mu_o A_g}\left\{(\phi_b+\phi_{cr})_I^2 - (\phi_b-\phi_{cr})_{III}^2\right\} + f_d \quad (1)$$

where

$$f_d = \left\{\left(\phi_{cx}^2\right)_I - \left(\phi_{cx}^2\right)_{III}\right\} \Big/ \mu_o A_g \quad (2)$$

means the destabilizing force induced by the axial control flux, that is, the coupled effect between radial and axial control. Here, $\mu_o\ (=4\pi\times10^{-7}\,H/m)$ is the permeability of free space and $A_g$ is the area of magnetic pole face. Subscripts *I* and *III* stand for the cores located in +*y* and –*y* directions, respectively. Fig. 3 shows a magnetic circuit model by each coil winding.

### A. *Case of uncoupled bias flux path(* $\phi_i = \phi_b + \phi_{cr}$ *)*

When the bias and radial control fluxes have an independent path, $\phi_i$ of Fig. 2(a) can be considered as $\phi_b$ + (or –) $\phi_{cr}$. Then, the magnetic flux in the upper and lower cores can be expressed as

$$(\phi_i)_{I,III} = (\phi_b+\phi_{cr})_{I,III} = (N_i I_i / R_r)_{I,III} = \mu_o A_g N_i (I_i/2g_o)_{I,III} \quad (3)$$

where $(g_o)_I = g_o - y$, $(g_o)_{III} = g_o + y$
$(I_i)_I = I_b + i_y$, $(I_i)_{III} = I_b - i_y$

Here, $N_i$ is the number of the inner coil turns, $I_b$ and $i_y$ are the bias and radial control currents, respectively, and

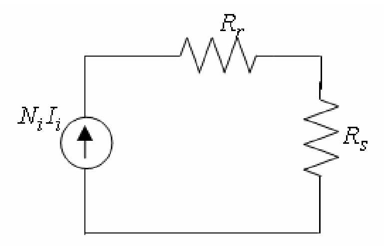


(a)

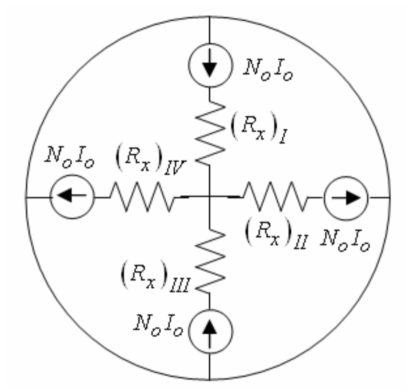


(b)

Fig. 3 Magnetic circuit models; (a) for inner coil, and (b) for outer coils

$g_o$ is the nominal air gap between stator and rotor.

Next, the axial control fluxes( $\phi_o = \phi_{cx}$ ) flow through the paths as depicted in Fig. 2(b). Its magnetic circuit can be simply modelled as Fig. 3(b). By using the Kirchhoff's law, the magnetic fluxes by axial control current can be calculated from

$$\frac{1}{2\mu_o A_g}\begin{bmatrix} 1 & -1 & 1 & -1 \\ g_o - y & g_o - z & 0 & 0 \\ g_o - y & 0 & 0 & g_o + z \\ 0 & g_o - z & g_o + y & 0 \end{bmatrix}\begin{bmatrix} (\phi_{cx})_I \\ (\phi_{cx})_{II} \\ (\phi_{cx})_{III} \\ (\phi_{cx})_{IV} \end{bmatrix} = \begin{bmatrix} 0 \\ 2N_o i_x \\ 2N_o i_x \\ 2N_o i_x \end{bmatrix} \tag{4}$$

Here, $N_o$ is the number of the outer coil turns, $i_x (= I_o)$ is the axial control current, and $y$ and $z$ is the small displacements in *y*- and *z*- directions, respectively. Solving (4), we can get the axial control fluxes going across the upper and lower air gaps as

$$(\phi_{cx})_I = \frac{2\mu_o A_g N_o i_x (g_o + y)}{2g_o^2 - y^2 - z^2} \tag{5}$$

$$(\phi_{cx})_{III} = \frac{2\mu_o A_g N_o i_x (g_o - y)}{2g_o^2 - y^2 - z^2} \tag{6}$$

Now, we can derive the force from (1), (3), (5) and (6). But, instead of showing the full equation here, we introduce its linearized form that is more useful for controller design. Assuming the control current and the rotor displacement are enough small compared with the bias current and the nominal air gap, the linearized form is obtained by using Taylor series expansion as

$$F_y \approx K_y y + K_{i_y} i_y + f_d \tag{7}$$

$$f_d = K_{rx} y \tag{8}$$

$$K_y = \frac{4\mu_o A_g N_i^2 I_b^2}{g_o^3},\ K_{i_y} = \frac{4\mu_o A_g N_i^2 I_b}{g_o^2},\ K_{rx} = \frac{4\mu_o A_g N_o^2 i_x^2}{g_o^3} \tag{9}$$

where $K_y$ and $K_{iy}$ are defined as the position stiffness and the current stiffness, respectively, just like a conventional AMB, and $K_{rx}$ is a destabilizing force generated by the axial control current, that is the coefficient of the coupled term. Note that $K_{rx}$ is independent from the radial displacement.

On the other hand, the Lorentz-type axial force can be determined by the magnetic field(bias flux density) of air gaps and the magneto-motive force(*mmf*) for axial control. Here, since the *mmf* (= $N_i I_b$) at the air gaps can be considered as a constant, so we need to adjust the magnetic field strength for generating the axial control force. The magnetic flux density and axial force can be given as

$$B_x = \frac{2N_o I_o}{R_x} = \frac{2N_o i_x}{R_x} = \frac{\mu_o N_o i_x}{g_o} \tag{10}$$

$$F_x = nB_x L N_i I_b = n\frac{\mu_o N_o N_i I_b L}{g_o} i_x \equiv K_{ix} i_x \tag{11}$$

where $L$ is the effective length of coil, $n$(= 4) is the number of cores generating the axial force, and $K_{ix}$ is the axial-direction current stiffness. Here, note that (11) is not a function of radial displacement.

## B. *Case of coupled bias flux path*

This is the case that the outer coil of Fig. 1 works for the radial control, which means $\phi_o = \phi_b + \phi_{cr}\ (or\ \phi_b - \phi_{cr})$, and the inner coil is used for the axial control. Since the path of the magnetic flux produced by the outer coil includes the adjacent cores, it is called the case that the bias fluxes are coupled. In this case, the magnetic fluxes at the air gaps can be obtained from

$$\begin{bmatrix} 1 & -1 & 1 & -1 \\ \frac{g_o - y}{2\mu_o A_g} & \frac{g_o - z}{2\mu_o A_g} & 0 & 0 \\ \frac{g_o - y}{2\mu_o A_g} & 0 & 0 & \frac{g_o + z}{2\mu_o A_g} \\ 0 & \frac{g_o - z}{2\mu_o A_g} & \frac{g_o + y}{2\mu_o A_g} & 0 \end{bmatrix}\begin{bmatrix} (\phi_o)_I \\ (\phi_o)_{II} \\ (\phi_o)_{III} \\ (\phi_o)_{IV} \end{bmatrix} = \begin{bmatrix} 0 \\ N_o(2I_b + i_y) \\ N_o(2I_b + i_y) \\ N_o(2I_b - i_y) \end{bmatrix} \tag{12}$$

That is,

$$(\phi_o)_I = \frac{\mu_o A_g N_o \left\{\left(2g_o^2 + 2g_o y\right) I_b + \left(2g_o^2 - g_o y - z^2\right) i_y\right\}}{g_o\left(2g_o^2 - y^2 - z^2\right)} \quad (13)$$

$$(\phi_o)_{III} = \frac{\mu_o A_g N_o \left\{\left(2g_o^2 - 2g_o y\right) I_b - \left(2g_o^2 + g_o y - z^2\right) i_y\right\}}{g_o\left(2g_o^2 - y^2 - z^2\right)} \quad (14)$$

On the other hands, the axial control flux( $\phi_i = \phi_{cx}$ )can be expressed by using magnetic circuit model of Fig. 3(a) as

$$\phi_{cx} = \frac{N_i I_i}{R_r} = \frac{\mu_o A_g N_i i_x}{2g_o} \quad (15)$$

Then, in a similar way as before, the linearized magnetic force is expressed again as

$$F_y \approx K_y y + K_{i_y} i_y + f_d \quad (16)$$

$$f_d = K_{rx} y \quad (17)$$

$$K_y = \frac{4\mu_o A_g N_i^2 I_b^2}{g_o^3},\ K_{i_y} = \frac{4\mu_o A_g N_i^2 I_b}{g_o^2},\ K_{rx} = \frac{4\mu_o A_g N_o^2 i_x^2}{g_o^3} \quad (18)$$

Here, it is important to make sure that these coefficients of linearized force equation are the very same as those of (9). This means that the above two cases can hold the controller design process in common, even if their operating principles are different from each other.

For the axial control, since the bias current for the radial control can be assumed to make the constant magnetic field, we can control the axial force by adjusting the current of inner coils. The bias magnetic flux density and the axial force(Lorentz force) can be given as

$$B_x = \mu_o N_o I_b / g_o \quad (19)$$

$$F_x = nB_x L N_i i_x = n\frac{\mu_o N_o N_i I_b L}{g_o} i_x \equiv K_{ix} i_x \quad (20)$$

Note that (20) is the same as (11), too.

## IV. Design of a Controller with Feedforward Loop

When a conventional 4-d.o.f. AMB controlled by a simple decentralized PD controller radially supports a rotor, the well-known equation of motion in the bearing fixed coordinate is written as

$$\boldsymbol{M}\ddot{\boldsymbol{q}} + K_s K_A \boldsymbol{K_d} \boldsymbol{K_i} \dot{\boldsymbol{q}} + \left(K_s K_A \boldsymbol{K_p} \boldsymbol{K_i} - \boldsymbol{K}\right)\boldsymbol{q} = \boldsymbol{f_d} \quad (21)$$

where $\boldsymbol{q} = \{y_1 \ \ y_2 \ \ z_1 \ \ z_2\}^T$ is a radial displacement vector of rotor at each bearing position, $\boldsymbol{M}$ is a mass matrix, $\boldsymbol{K}$ and

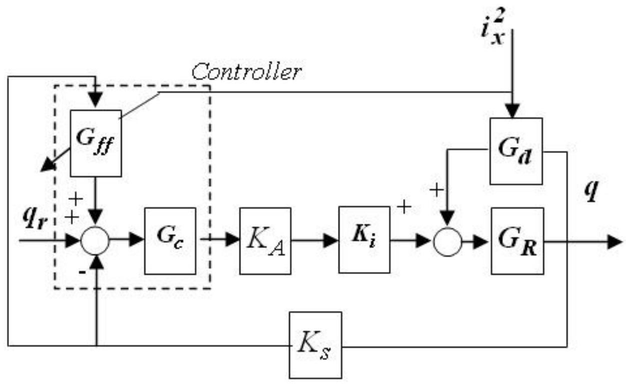


Fig. 4 Block diagram for radial controller with a feedforward loop

$\boldsymbol{K_i}$ are the position stiffness and the current stiffness matrices which are concerned with the first and the second coefficients of (9) or (18), respectively, $K_s$ and $K_A$ are the displacement sensor gain and the power amplifier gain, respectively, and $\boldsymbol{K_p}$ and $\boldsymbol{K_d}$ are the proportional and the derivative gain matrices. Generally $\boldsymbol{f_d}$ is a disturbance term but here, it means the destabilizing force caused by axial control flux.

For the proposed AMB, a radial controller was designed based on (21), but a feedforward loop was added for compensation of $\boldsymbol{f_d}$. Fig. 4 shows the block diagram; $\boldsymbol{G_c}$ and $\boldsymbol{G_R}$ are the transfer functions of PD controller and the uncontrolled rotor system; $\boldsymbol{G_d}$ is the disturbance concerned with (8) or (17); and $\boldsymbol{G_{ff}}$ is the transfer function of the feedforward controller to get rid of the effect of $\boldsymbol{G_d}$, which is determined as

$$\boldsymbol{G_{ff}} = -\left(K_s K_A \boldsymbol{K_i} \boldsymbol{G_c}\right)^{-1} \boldsymbol{G_d} \quad (22)$$

In (22), note that the transfer functions $\boldsymbol{G_d}$ and $\boldsymbol{K_i}$ are accurately modeled, the deterministic disturbance $\boldsymbol{G_d}$ caused by the axial control current can be well compensated. In addition, even if it is hard to obtain the accurate model, it is not so serious because the existence of axial control flux can be regarded as a small variation of the bias flux.

On the other hand, the axial controller design is simpler. Neglecting the derivation process, we can write the equation of motion including the PD controller as

$$m\ddot{x} + nK_s K_A K_{dx} K_{ix} \dot{x} + nK_s K_A K_{px} K_{ix} x = 0 \quad (23)$$

Here, $m$ is the rotor mass and $K_{px}$ and $K_{dx}$ are the proportional and derivative gains, respectively. Unlike general AMBs, (23) doesn’t include the position stiffness term, which means that it is marginally stable(or passively stable depending on the radial stability) even without any controller. It is a good point of Lorentz-type AMB.

## V. Experimental Setup and Results

Prior to the experiment, some FEM analyses were performed to predict the feasibility of the proposed AMB. Fig. 5 shows a plot of the control current versus axial

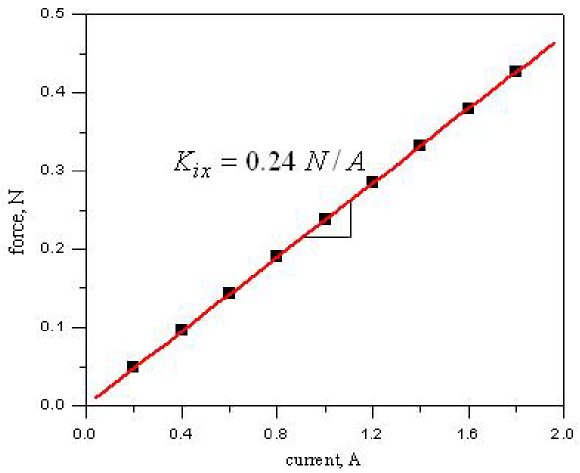


Fig. 5 FEM analysis results: axial control current versus force

magnetic force. The linearity of the figure meets the characteristics of Lorentz force well and its slope stands for the current stiffness $K_{ix}$ in $x$ direction.

The experimental system consists of AMB units developed in laboratory, five eddy-current-type proximity probes, a digital controller using a Power-PC board (dSPACE Inc., DS1103), and a 9-channel linear power amplifier. Radial displacements of the rotor measured by

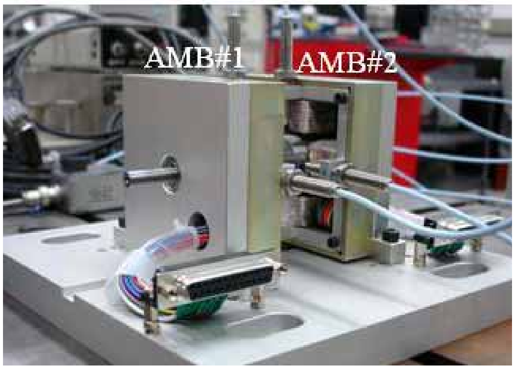


(a)

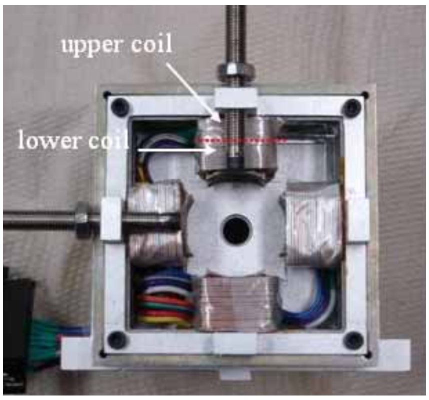


(b)

Fig. 6 (a) Prototype of the proposed AMB and (b) its stator structure

TABLE I
SPECIFICATION OF THE PROTOTYPE

| Parameter | | Value |
|---|---|---|
| pole face area | | 102 mm$^2$ |
| air gap | | 0.4 mm |
| coil turn | upper | 60 |
| | lower | 60 |
| position stiffness | | $4.87\times10^4$ N/m |
| current stiffness | | 15 N/A |
| mass | | 0.28 kg |
| bias current | | 1.3 A |

proximity probes are input to the control board of the host PC and 12-bit A/D converted at the sampling frequency of 5 kHz. The control currents from the power amplifier are fed to coils, producing the radial and axial electromagnetic forces.

Fig. 6 shows the prototype integrated AMB. Two bearing planes support the rotor and a U-shaped core on stator has double-layer coils. The specification of the designed AMB is listed in TABLE I. The proposed AMB has the capability of 3-d.o.f control with only one magnetic bearing unit, and we built 5-d.o.f AMB system with two bearing planes.

Fig. 7 to Fig. 10 compare impulse responses of the controlled AMB when the levitated rotor(not rotated) is impacted in axial($x$) and radial($y$, $z$) directions for the two proposed control configuration. In the controlled AMB, the oscillation by impact are damped out in 0.3 sec and 0.2 sec about $x$- and $y$-direction, respectively. While, the settling times in uncontrolled axial responses were found to 28 sec and 30 sec, respectively. The axial uncontrolled and controlled eigenvalues are estimated to be

$$\lambda_{uc1,2} = -0.28 \pm 30.7\,j \text{ and } \lambda_{c1,2} = -25.6 \pm 82.7\,j$$

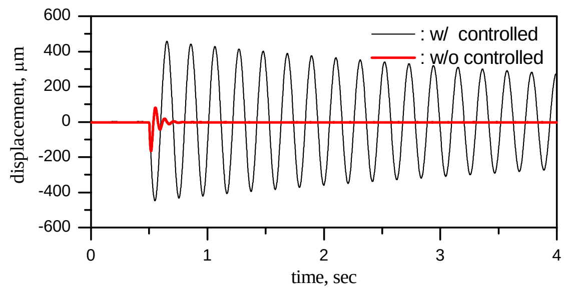


(a) $x$-direction

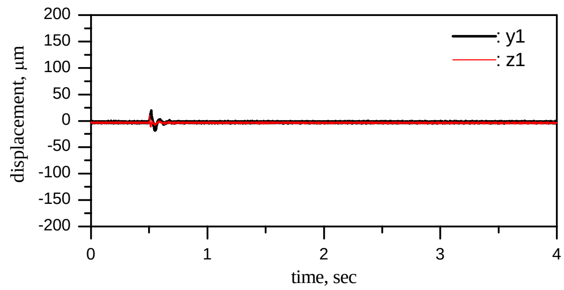


(b) $y_1$ and $z_1$ direction

Fig. 7 Responses to $x$-directional impulse under independent radial control

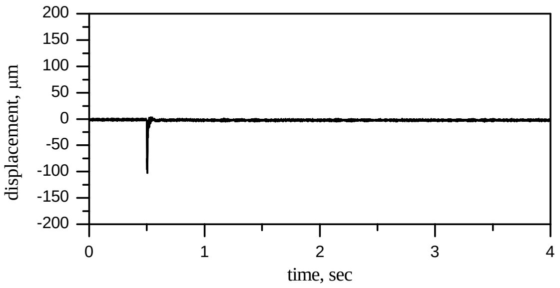

(a) $y$ direction

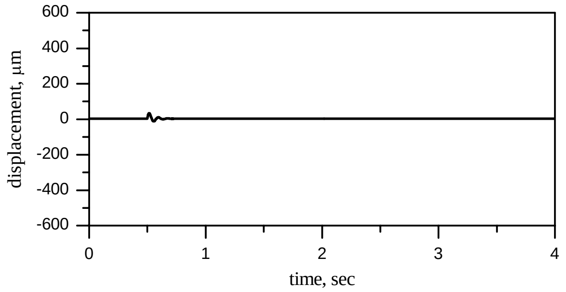

(b) $x$ direction

Fig. 8 Responses to $y$ directional impulse under independent radial control

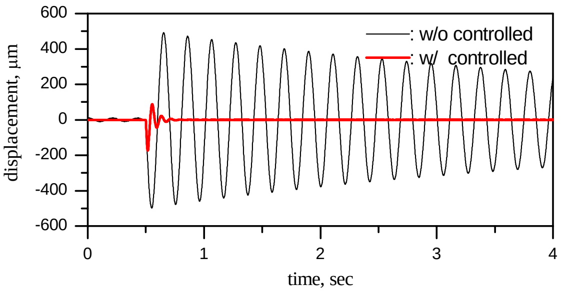

(a) $x$ direction

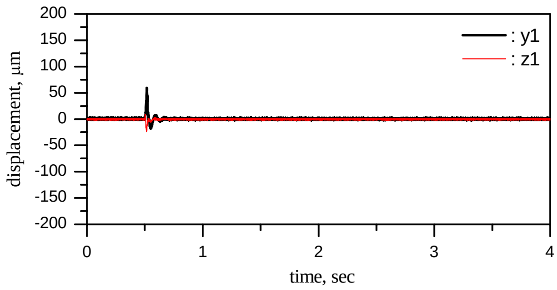

(b) $y_1$ and $z_1$ direction

Fig. 9 Responses to $x$ directional impulse under coupled radial control

in the independent bias flux type and

$$\lambda_{uc1,2} = -0.11 \pm 31.3j \text{ and } \lambda_{c1,2} = -24.8 \pm 81.6j$$

in the coupled bias flux type. One can see that the feedforward control loop effectively compensates for the disturbance by the axial control current at the radial control.

## VI. Conclusions

We proposed a new compact AMB system that had the integrated radial and axial bearing without the axial disk. Its has some merits: most of all, it is possible to design a small-size AMB, and it has two kinds of operating principle which are modelled in the same equation of motion and thus can use the same controller. This means the role of each coil can be switched in an emergency even during the operation. The feasibility of the proposed AMB was experimentally verified for both of the proposed principles.

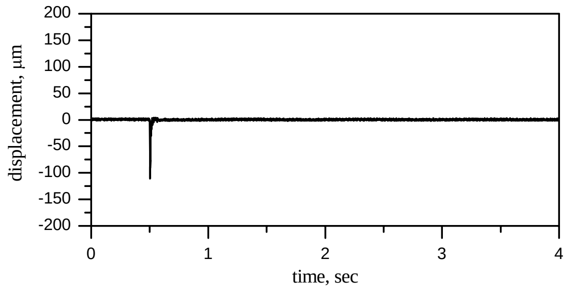

(a) $y$ direction

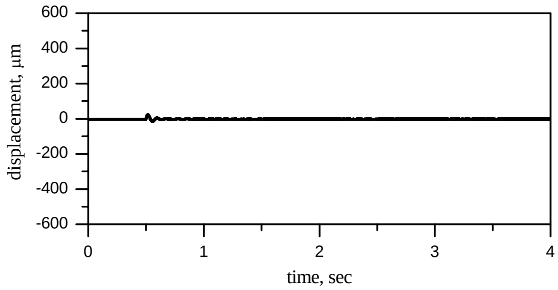

(b) $x$ direction

Fig.10 Responses to $y$ directional impulse under coupled radial control

## References


[1] C. W. Lee, and H. S. Jeong, "Dynamic modelling and optimal control of cone-shaped active magnetic bearing system," Control Engineering Practice, vol. 4, pp.1393~1403, 1996.

[2] A. M. Mohamed, and F. P. Emad, "Conical magnetic bearings with radial and thrust control," IEEE Transactions on Automatic Control, vol. 37, no. 12, pp.1859~1868, 1992.

[3] J. P. Yonnet, "Passive magnetic bearings with permanent magnets," IEEE Transactions on Magnetics, vol. 14, no. 5, pp.803~805, 1978.

[4] M. Komori, and T. Yamane, "Magnetic levitation system with a millimeter sized cylindrical rotor," Mechatronics, vol. 10, pp.595-607, 2000.

[5] H. Y. Kim, and C. W. Lee, "Design and Control of Active Magnetic Bearing System with Lorentz Force-type Axial Actuator," ASME2003 Design Engineering Technical Conferences and Computers and Information in Engineering Conference, Chicago, Illinois, USA, September 2003, 48542.

[6] N. Kurita, Y. Okada, and K. Matsuda, "Development of Lossless Magnetic Bearing," 8th Int. Sym. on Magnetic Bearings, Mito, Japan, pp.91~96, 2002.